

Hybrid Open Networks (MIL 16): Synthesis, Crystal Structure, and Ferrimagnetism of $\text{Co}_4(\text{OH})_2(\text{H}_2\text{O})_2(\text{C}_4\text{H}_4\text{O}_4)_3 \cdot 2\text{H}_2\text{O}$, a New Layered Cobalt(II) Carboxylate with 14-Membered Ring Channels

Carine Livage, Chrystelle Egger, and Gérard Férey*

*Institut Lavoisier (UMR CNRS 8637), Université de Versailles St-Quentin,
45 av. des Etats-Unis, 78035 Versailles, France*

Received December 16, 1998. Revised Manuscript Received March 1, 1999

A new layered cobalt succinate, $\text{Co}_4(\text{OH})_2(\text{H}_2\text{O})_2(\text{C}_4\text{H}_4\text{O}_4)_3 \cdot 2\text{H}_2\text{O}$, was prepared under hydrothermal conditions at 180 °C from a 1:1.5:4:120 mixture of Co(II) chloride hexahydrate, succinic acid, potassium hydroxide, and water. The structure was solved by single-crystal X-ray diffraction: $P\bar{1}$, $a = 10.181(2)$, $b = 10.668(2)$, $c = 12.857(2)$ Å, $\alpha = 112.97(3)^\circ$, $\beta = 91.24(3)^\circ$, $\gamma = 117.96(3)^\circ$, $V = 1099.1(4)$ Å³, $Z = 2$, 5511 F^2 values with $I = 2\sigma(I)$, $R1 = 0.045$ and $wR2 = 0.114$. The title compound presents a structure constituted by the stacking along [100] of metal oxide layers in which 14-membered ring windows appear. Succinate anions linked the cobalt atoms within each layer. From magnetization measurements, this compound is ferrimagnetic below 10 K.

Introduction

The use of organic moiety is actually the most promising route to tailor properties and topologies of transition metal compounds.^{1–3} With the hydrothermal technique, the templating effect of organic cations (ammonium ions) has allowed the development of the chemistry of microporous compounds.^{4–5} Those compounds present an anionic inorganic framework, charge-compensated by cationic organic guests in the cavities of the solid. The problem with the practical use of these phases is the difficulty in removing the organic template from the cavities without altering the framework. One strategy for expanding the structural chemistry of open frameworks is to use phosphonate or diphosphonate, the organic moiety being used to space out the transition metal.^{6–8} Traditionally carboxylate anions have been used in the coordination chemistry to tailor the properties of single metal cations or small groups of ions. We are currently interested in the use of the complexing properties of carboxylic acids to build open structure materials.^{9–12} Under hydrothermal conditions, carboxylate is part of the framework and leads to the formation

of neutral open networks with only water as “host” molecules. The efficiency of this method was recently evidenced by the preparation of $\text{Co}_5(\text{OH})_2(\text{C}_4\text{H}_4\text{O}_4)_4$, a cobalt carboxylate with a three-dimensional structure built up from layers that formed 12-membered ring windows, pillared by succinate ions.¹² We present here the synthesis of $\text{Co}_4(\text{OH})_2(\text{H}_2\text{O})_2(\text{C}_4\text{H}_4\text{O}_4)_3 \cdot 2\text{H}_2\text{O}$, a new cobalt carboxylate with a two-dimensional array of edge-sharing Co^{2+} octahedra and a large ring defined by 14 cobalt polyhedra. This compound has been fully characterized by FT-IR spectroscopy, microanalysis, thermal analysis, magnetic measurements, and powder and single-crystal X-ray diffraction. $\text{Co}_4(\text{OH})_2(\text{H}_2\text{O})_2(\text{C}_4\text{H}_4\text{O}_4)_3 \cdot 2\text{H}_2\text{O}$ is denoted MIL-16 for Materials of Institut Lavoisier.

Experimental Section

Materials and Methods. Hydrothermal reactions were carried out in 23-mL Teflon-walled Parr acid digestion bombs. X-ray powder diffraction data were collected on a Siemens D5000 diffractometer with Cu K α radiation for room-temperature measurements and Co K α for temperature-dependent measurements (50–210 °C). X-ray single-crystal diffraction data were collected on a Siemens SMART diffractometer with Mo K α radiation. FT-IR spectra were recorded on a Nicolet Magna-IR 550 spectrometer. Thermogravimetric analyses were done using a TA-Instruments TGA-2050 apparatus (oxygen gas flow, 60 mL/min; 5 °C/min and 10 °C/min), and the studies of thermal exchanges, on a TA-Instrument DSC-2010 calorimeter (oxygen gas flow 60 mL/min, 5 °C/min and 10 °C/min). Magnetization measurements were carried out using a Quantum Design Squid magnetometer. The data were not corrected for the core diamagnetism, which represent less than 1% of the signal. The values of the standard deviations range from 10^{-8} emu (21 K, 100 G) to $7 \cdot 10^{-4}$ emu (2 K, 5000 G), which correspond to less than 1% of the signal.

Synthesis and Characterization of $\text{Co}_4(\text{OH})_2(\text{H}_2\text{O})_2(\text{C}_4\text{H}_4\text{O}_4)_3 \cdot 2\text{H}_2\text{O}$. $\text{Co}_4(\text{OH})_2(\text{H}_2\text{O})_2(\text{C}_4\text{H}_4\text{O}_4)_3 \cdot 2\text{H}_2\text{O}$ was hydrothermally synthesized from a mixture composed of cobalt(II) chloride hexahydrate, succinic acid, potassium hydroxide, and

- (1) Férey, G. *C. R. Acad. Sci. Ser. C* **1998**, *1*.
- (2) Day, P. *J. Chem. Soc., Dalton Trans.* **1997**, 701.
- (3) Decurtins, S.; Schmalke, H. W.; Pellaux, R.; Hauser, A.; von Arx, M. E.; Fischer, P. *Synth. Met.* **1997**, *85*, 1689.
- (4) Feng, P.; Bu, X.; Stucky, G. D. *Nature* **1997**, *388*, 735.
- (5) Debord, J. R.; Haushalter, R. C.; Zubietta, J. J. *Solid State Chem.* **1996**, *125*, 270.
- (6) Drumel, S.; Janvier, P.; Bujoli-Doeuff, M.; Bujoli, B. *Inorg. Chem.* **1996**, *35*, 5786.
- (7) Lohse, D. L.; Sevov, S. C. *Angew. Chem., Int. Ed. Engl.* **1997**, *36* (15), 1619.
- (8) LaDuca, R.; Rose, D.; DeBord, J. R. D.; Haushalter, R. C.; Connor, C. J. O.; Zubietta, J. J. *Solid State Chem.* **1996**, *123*, 408.
- (9) Distler, A.; Sevov, S. *Chem. Commun.* **1998**, 959.
- (10) Gutschke, S. O. H.; Molinier, M.; Powell, A. K.; Wood, P. T. *Angew. Chem., Int. Ed. Engl.* **1997**, *36* (9), 991.
- (11) Serpaggi, F.; Férey, G. *J. Mater. Chem.* **1998**, *8*, 2737.
- (12) Livage, C.; Egger, C.; Nogues, M.; Férey, G. *J. Mater. Chem.* **1998**, *8*, 2743.

Table 1. Summary of Crystal Data and Structure Refinement

space group	$P\bar{1}$
<i>a</i> , Å	10.181(2)
<i>b</i> , Å	10.668(2)
<i>c</i> , Å	12.857(3)
α , deg	112.97(3)
β , deg	91.24(3)
γ , deg	117.96(3)
<i>V</i> , Å ³ ; <i>Z</i>	1099.1(4), 2
calculated density, g/cm ³	2.085
absorption coefficient, mm ⁻¹	3.053
<i>F</i> (000)	692
θ range for data collection, deg	1.78–29.81
limiting indices	$-14 \leq h \leq 13$, $-8 \leq k \leq 14$, $-16 \leq l \leq 17$
reflections collected	7803
independent reflections	5511
data, restraints, parameters	5511, 0, 377
goodness-of-fit on <i>F</i> ²	1.003
final <i>R</i> indices [<i>I</i> > 2 σ (<i>I</i>)]	<i>R</i> 1 = 0.0450, <i>wR</i> 2 = 0.1143
final <i>R</i> indices all data	<i>R</i> 1 = 0.0504, <i>wR</i> 2 = 0.1166
largest diff. peak and hole, e/Å ³	1.114 and -1.337

water in the molar ratios 1:1.5:4:120. The starting mixture was heated 3 days at 180 °C under autogenous pressure (initial pH 3.6, final pH 5.5). The resulting solid phase was filtered off and dried at room temperature. It consists of pink plates of the title compound. In contrast to the synthesis of Co₅(OH)₂-(C₄H₄O₄)₄ which can be prepared under various conditions¹² (varying the concentration, duration, and nature of reactants) the preparation of Co₄(OH)₂(H₂O)₂(C₄H₄O₄)₃·2H₂O requires very strict conditions. A single crystal was used for the structure determination by X-ray diffraction. The X-ray powder diffraction pattern agrees with that calculated from the refined structure. IR spectra exhibited the following absorption (KBr pellet; ν , cm⁻¹): a broad band due to the presence of water molecules, ν (O–H) 3430; ν (C–H) stretching bands characteristic of CH₂ groups between 2900 and 3000; four peaks at 1635, 1560, 1445, and 1405 due to the carboxylic groups (C=O and C–O); and the following bands, 1220, 1175, 930, and 670 which are not attributed for certain. Elemental analysis confirmed the composition of the solid with experimental values (mass percent) of C 19.9; H 3.1; and Co 34.1 and calculated ones of C 20.9; H 3.2; and Co 34.2.

Single-Crystal Structure Determination. A selected crystal (0.5 × 0.2 × 0.1 mm) of Co₄(OH)₂(H₂O)₂(C₄H₄O₄)₃·2H₂O was glued to a glass fiber and mounted on a SMART three-circle diffractometer with a CCD two-dimensional detector. By using monochromatic molybdenum radiation (λ Mo K α = 0.7107 Å), intensity data were collected in 1271 frames with ω scans (width of 0.30° and exposure time 30 s per frame). A summary of crystal data is presented in Table 1. The data collected were corrected for Lorentz, polarization, and absorption effects using the SADABS program.¹³ The structure was solved by direct methods and refined by full matrix least squares, based on *F*², using the SHELX-TL software package.¹⁴ Cobalt and oxygen atoms were located first and all the remaining atoms, including hydrogen atoms, were found by difference Fourier maps. All the residual electronic density (<1.2 e/Å³) is located near Co atoms. The refinement was performed using anisotropic thermal parameters for all non-hydrogen atoms. Isotropic displacement factors were fixed at the value of 0.05 Å² for all hydrogen atoms. The compound contains four water molecules: two are coordinating a cobalt atoms [Co(5)–OW1 and Co(5)–OW2] and two are located in the channels (OW3 and OW4). The thermal parameter of OW4, which presents only one significant hydrogen interaction [O(13)–H···OW4], is larger than the others (equivalent iso-

Table 2. Atomic Coordinates (10⁻⁴) and Equivalent Displacement Parameters (10⁻³ Å²) for Non-hydrogen Atoms

atom	<i>x</i>	<i>y</i>	<i>z</i>	<i>U</i> _{eq} ^a
Co(1)	7996(1)	3452(1)	1490(1)	17(1)
Co(2)	9812(1)	3955(1)	3701(1)	18(1)
Co(3)	0	5000	0	18(1)
Co(4)	5000	0	0	20(1)
Co(5)	7501(1)	5099(1)	4317(1)	21(1)
O(1)	5850(3)	-308(3)	1266(2)	31(1)
O(2)	8090(3)	1981(3)	2215(2)	23(1)
O(3)	537(3)	2744(3)	4292(2)	24(1)
O(4)	1005(3)	941(3)	4345(2)	35(1)
O(5)	8127(2)	4838(3)	682(2)	22(1)
O(6)	6781(3)	5869(4)	1605(2)	36(1)
O(7)	1460(3)	4243(3)	2673(2)	27(1)
O(8)	285(2)	4289(3)	1237(2)	22(1)
O(9)	5634(2)	2279(3)	1269(2)	22(1)
O(10)	5465(3)	3129(3)	3107(2)	38(1)
O(11)	1277(3)	7400(3)	1173(2)	30(1)
O(12)	7271(2)	1453(3)	-165(2)	22(1)
O(13)	8456(2)	4089(3)	4875(2)	20(1)
O(14)	8860(2)	5041(3)	3165(2)	18(1)
OW1	6774(3)	6428(3)	3891(2)	31(1)
OW2	6299(3)	5096(4)	5627(2)	38(1)
C(1)	7076(3)	589(4)	2051(2)	22(1)
C(2)	7389(4)	-7(4)	2859(3)	33(1)
C(3)	8913(5)	24(5)	2853(4)	42(1)
C(4)	10241(4)	1319(4)	3911(3)	24(1)
C(5)	7384(3)	5560(4)	795(3)	22(1)
C(6)	7282(5)	6099(5)	-122(3)	34(1)
C(7)	2923(4)	5048(5)	1379(3)	31(1)
C(8)	1462(3)	4491(4)	1800(2)	21(1)
C(9)	4886(3)	2403(3)	2050(3)	21(1)
C(11)	7615(5)	-154(4)	-1920(3)	38(1)
C(10)	3169(4)	1567(4)	1648(3)	27(1)
C(12)	7858(3)	1402(4)	-1021(2)	21(1)
OW3	1006(4)	8097(4)	3469(3)	44(1)
OW4	3609(6)	8337(6)	4437(5)	96(2)

^a *U*_{eq} is defined as one-third of the trace of the orthogonalized *U*_{ij} tensor.

Table 3. Selected Bond Lengths (Å) and Angles (deg)

Co(1)–OH(14)	1.989(2)	Co(3)–O(11)	2.074(3)
Co(1)–O(5)	2.074(2)	Co(3)–O(8)	2.078(2)
Co(1)–O(9)	2.075(2)	Co(3)–O(5)	2.077(2)
Co(1)–O(12)	2.129(2)	Co(4)–O(1)	2.033(2)
Co(1)–O(2)	2.149(2)	Co(4)–O(9)	2.092(2)
Co(1)–O(8)	2.154(2)	Co(4)–O(12)	2.170(2)
Co(2)–OH(13)	2.060(3)	Co(5)–OH(13)	2.044(2)
Co(2)–OH(13)	2.075(2)	Co(5)–OH(14)	2.052(2)
Co(2)–OH(14)	2.099(2)	Co(5)–O(10)	2.087(3)
Co(2)–O(2)	2.101(3)	Co(5)–OW2	2.103(3)
Co(2)–O(3)	2.103(2)	Co(5)–OW1	2.106(3)
Co(2)–O(7)	2.142(2)	Co(5)–O(3)	2.193(3)
Co(2)–O(2)–Co(1)	92.60(9)	Co(5)–OH(13)–Co(2)	101.48(10)
Co(2)–O(3)–Co(5)	95.39(9)	Co(5)–OH(13)–Co(2)	98.05(9)
Co(1)–O(5)–Co(3)	99.48(9)	Co(2)–OH(13)–Co(2)	97.07(9)
Co(3)–O(8)–Co(1)	96.94(9)	Co(1)–OH(14)–Co(5)	121.91(11)
Co(1)–O(9)–Co(4)	100.42(10)	Co(1)–OH(14)–Co(2)	97.44(10)
Co(1)–O(12)–Co(4)	96.21(9)	Co(5)–OH(14)–Co(2)	97.06(9)

tropic displacement of 0.09 Å²). Fractional atomic coordinates are given in Table 2 and selected bond lengths and angles in Table 3.

Results and Discussion

Structural Description of Co₄(OH)₂(H₂O)₂(C₄H₄O₄)₃·2H₂O. A major feature of the structure is a two-dimensional network of edge-sharing cobalt octahedra (Figure 1). Connection of the polyhedra forms 14-membered ring windows, in which four weakly bonded water molecules are incorporated. The succession of the layers formed hydrated channels along the [100] direction (Figure 2). Each succinate anion links, by oxygen–

(13) Sheldrick, G. M. *SADABS; Program for scaling and correction of area detector data*; University of Göttingen: Göttingen, Germany, 1997.

(14) Sheldrick, G. M. *Acta Crystallogr.* **1990**, *A46*, 467; *SHELX-TL version 5.03, Software Package for the Crystal Structure Determination*; Siemens Analytical X-ray Instrument Division: Madison, WI, 1994.

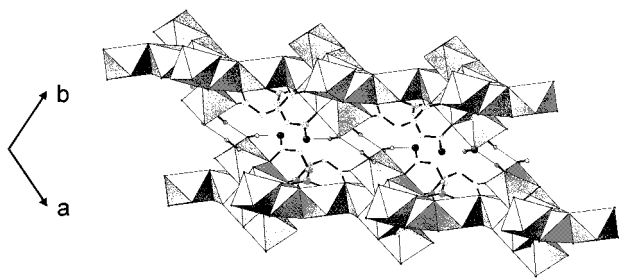


Figure 1. Projection of the structure along [001]. Cobalt layers are represented by edge-sharing octahedra and the alkyl chain in the ball-and-stick mode. Gray spheres are carbon atoms and black spheres terminal oxygen atoms. Thin lines correspond to hydrogen bonds.

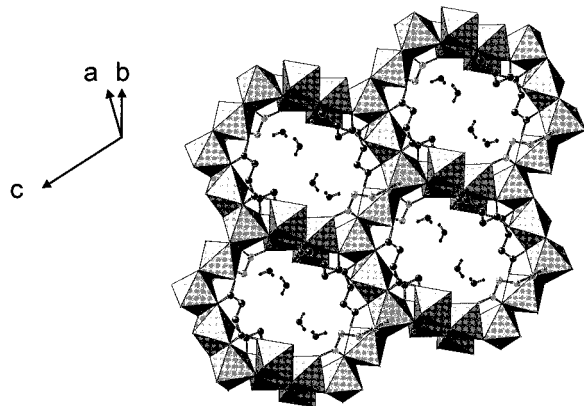


Figure 2. Projection of one layer. Organic alkyl chains are represented by a ball-and-stick mode: black spheres, C(1)–C(4); light gray spheres, C(5)–C(8); and dark gray spheres, C(9)–C(12). Water molecules are represented in black.

metal bonds, four cobalt atoms within the layers. Therefore, the organic molecules are part of the layers. No covalent bond links adjacent layers and the three-dimensional arrangement of the structure is ensured by weak interactions. Cobalt atoms occupy five different crystallographic sites. Coordination of cobalt atoms has a slightly distorted octahedral geometry with Co–O bonds ranging from 1.989 to 2.192 Å. Co(3) and Co(4) are coordinated by oxygen atoms from succinate ions; Co(1) and Co(2), from succinate ions and hydroxyl groups; and Co(5), from succinate ions, hydroxyl groups, and two water molecules. Each succinate anion is a bidentate ligand for one cobalt atom. The presence of two terminal hydroxyl groups and two coordinated water molecules is consistent with valence sum calculations.¹⁵ As in many other transition metal oxides, the hydroxide oxygen atoms, O(13) and O(14), are shared by three cobalt atoms with Co– μ_3 -O(H) bonds between 1.989 and 2.098 Å.⁶ The two coordinated water molecules (OW1, OW2) participate in the cohesion of the structure with strong hydrogen bonds between layers [Co–OW2–H \cdots OW1–Co; 2.203 Å]. The layers contain approximately ovoid windows of 14 Co²⁺ octahedra linked by the organic molecules (Figure 3). The approximate dimensions of the cavities are 9.6 and 7.4 Å (C \cdots C distances). Water molecules located into the cavities are linked to the network by hydrogen bonds: OW3 presents three strong hydrogen bonds [O(14)–H \cdots OW3, 2.04 Å; OW3–H \cdots O(4), 1.90 Å; and OW3–H \cdots

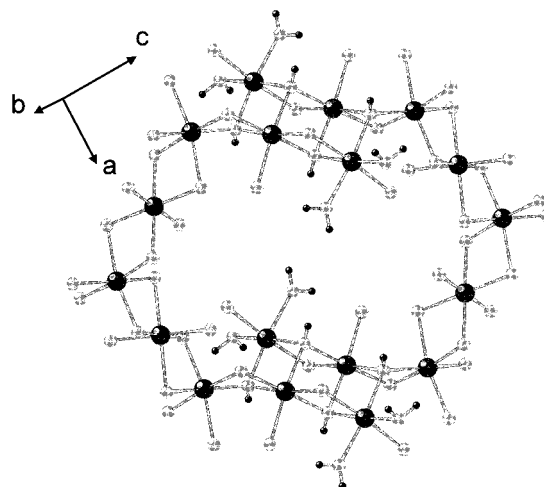


Figure 3. Connectivity of the Co²⁺, {CoO₆} octahedra. Small black spheres correspond to hydrogen atoms of the hydroxyl group and coordinated water molecules.

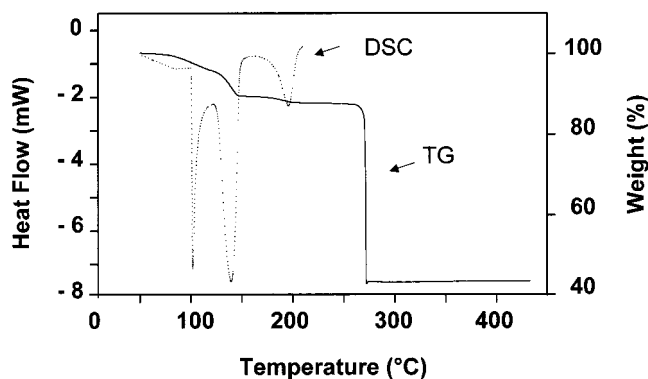


Figure 4. Thermal behavior of Co₄(OH)₂(H₂O)₂(C₄H₄O₄)₃·2H₂O, TG, and DSC curves showing the weight loss and thermal exchanges upon heating.

O(11), 1.95 Å], and OW4, which is more agitated, presents only one hydrogen bond [O(13)–H \cdots OW4, 2.21 Å].

Thermal Behavior. The thermal behavior of the title compound was studied by thermal analysis (TG, DSC) and X-ray powder diffraction (XRD) upon heating. These experiments showed that Co₄(OH)₂(H₂O)₂(C₄H₄O₄)₃·2H₂O undergoes two decompositions, characterized by the loss of water molecules, before deteriorating due to the combustion of the organic moiety. The TG and DSC curves are presented in Figure 4, and XRD patterns, recorded during a dehydration–rehydration process (50–210 °C and 210–50 °C), in Figure 5. The TG results showed the mass loss of approximately five water molecules, whereas the structure determination reveals only four. The initial weight loss (100 and 140 °C, endothermic peaks) corresponds to the mass loss of four water molecules (theoretical weight loss 10.4%, observed 10.7%). Coordinated water molecules being removed, this modification leads to a change in the coordination sphere of Co(5) that can be visualized by the change of color of the compound, which from pink becomes blue-violet. The reversibility of this transition is not visible for the condition of the XRD experiment upon heating (Figure 5). However, the dehydration is reversible and the color of the compound turns pink again in air (~30 min.). TG trace of the rehydrated solid (1 h in air) is similar to that of the initial product showing that the compound is able to readsorb four water molecules. In

(15) Brese, N.; O'Keeffe, M. *Acta Crystallorg.* **1991**, B47, 192.

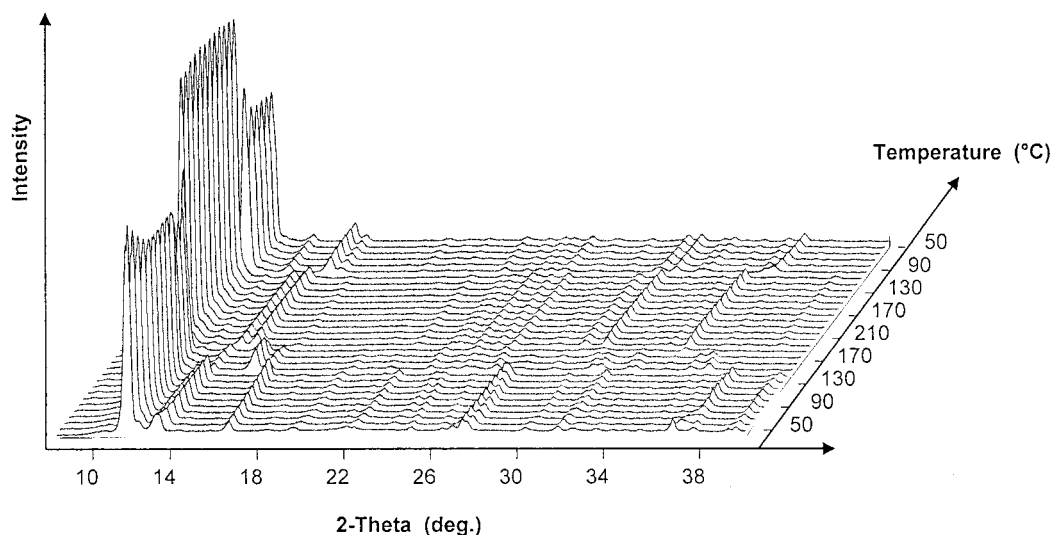


Figure 5. Powder X-ray diffraction patterns versus temperature (Co K α) showing the crystalline phase transitions upon dehydration–rehydration processes (50 °C–210 °C–50 °C).

agreement, XRD pattern of the rehydrated powder corresponds to that of the initial compound. A second phase transition, around 190 °C, is accompanied by an endothermic weight loss (weight loss of one water molecule 2.5%, observed 1.9%). This process is not yet understood. However, considering the structure, it is probably due to a structural reorganization that involves the hydroxide groups. As seen on the XRD patterns, this last transformation is reversible and a “rehydration” appears around 100 °C (exothermic on DSC). Structural determination of the dehydrated products is currently being investigated. The last stage on the TG trace, an abrupt weight loss at 275 °C, is characteristic for the combustion of the organic moiety (exothermic, theoretical weight loss 45.2%, observed 44.3%). The resulting product at 300 °C is, according to XRD, CoO.

Magnetic Properties. Magnetic properties of oxide materials depend essentially on metal–oxygen–metal linkages. The network of cobalt octahedra (d^7) can be described as parallel “helical” chains along [010], of Co^{2+} octahedra sharing edges, linked to each other by tetrameric units constituted by four coplanar octahedra with a rhomboid-like geometry. Figure 6 illustrates the Co^{2+} octahedron arrangement (angles Co–O–Co between 95.5 and 101.5°, Co···Co distances between 3.10 and 3.18 Å). The temperature dependence of the $1/\chi_m$ (100 G), is shown in Figure 7 with the magnetization versus the applied magnetic field at 2 K. Above 50 K, the data follow the Curie–Weiss law with $C = 13.3 \text{ emu mol}^{-1}$ and $\theta_p = -20.8 \text{ K}$. This gives a magnetic moment of $5.2 \mu_B$ per atom, which is commonly observed¹⁶ for independent Co^{2+} centers even if this value is larger than the spin-only value of $3.88 \mu_B$. Around 25 K a change in the $1/\chi_m(T)$ curve, characterized by an increase of susceptibility, indicates a magnetization confirmed by the $M(H)$ curve below the critical temperature ($\sim 10 \text{ K}$). The experimental value of the magnetization at high field (5.5 T) is close to $6 \mu_B$ per mole, which corresponds to 2μ (Co^{2+}). A possible model for the magnetic structure can be proposed from these values and the structural characteristics of the title com-

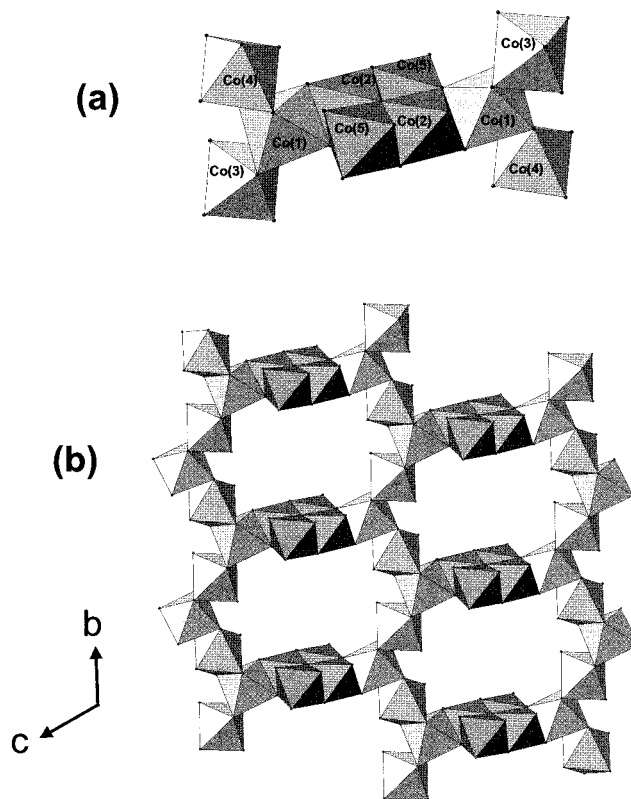


Figure 6. (a) Vicinities of cobalt atoms and (b) polyhedral representation showing the connectivity between cobalt octahedra within the tetrameric unit (gray polyhedra) and the helical chain (white polyhedra). Alkyl chains and water molecules have been omitted for clarity.

pound: an antiferromagnetic coupling within the Co(1)–Co(3)–Co(4) helical (or cis–trans) chain and ferromagnetic coupling in the tetramer. The latter has been already encountered either in three-dimensional or molecular solids. Neutron diffraction studies of $\text{Ba}_2\text{Ni}_7\text{F}_{18}$,¹⁷ $\text{Ba}_2\text{Co}_7\text{F}_{18}$,¹⁸ and Co^{2+} containing polyoxometalates^{19,20} show that ferromagnetic coupling occurs within the tetrameric unit. More surprising would be the

(16) Carlin, R. L. *Magnetochemistry*; Springer-Verlag: Berlin, New York, 1986.

(17) Renaudin, J.; Férey, G.; de Kozak, A.; Samouël, M.; Lacorre, P. *Solid State Commun.* **1988**, *65*, 185.

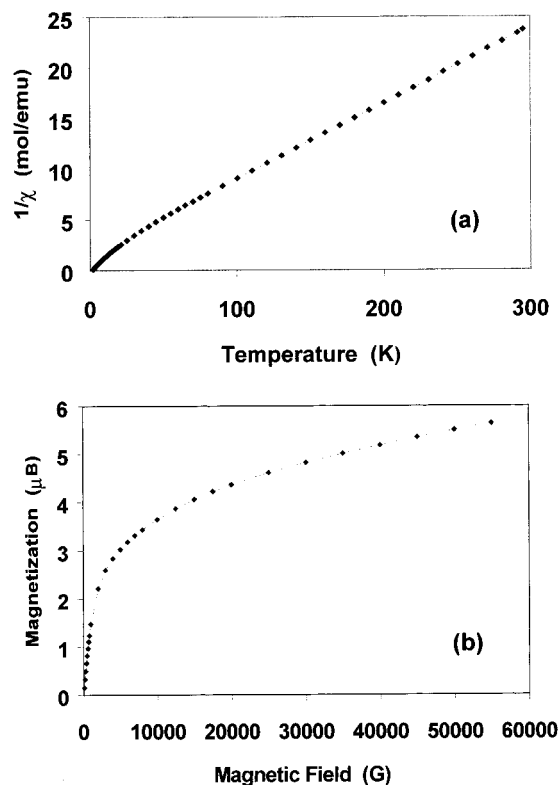


Figure 7. (a) Temperature dependence of $1/\chi_m$ and (b) magnetization data versus the applied field at 2 K.

antiferromagnetic interactions within the chains in which, as in the cluster, edge sharing of polyhedra occur. It is well-known that in 90° superexchange interactions, small variations of the angle around the superexchange "blank angle" can invert the sign of the coupling constant (~ 90 – 100° , depending on the nature of the 3d transition metal cation).²¹ Large superexchange angles lead to antiferromagnetic interactions while weaker ones induce ferromagnetic coupling. Moreover, the exchange constant J of the exchange Hamiltonian ($H = -\sum J_{ij} S_i \cdot S_j$) has small values in this region and this can explain the low T_C of the title compound. Within the chain, it is clear that the most efficient magnetic exchange pathways will correspond to the shortest Co–O distances. Common Co–O distances are about 2.1 Å in Co^{2+}O_6 octahedra, which is more or less the average value observed for the octahedra of the structure. In the "helicoidal" chains, Co(4) and Co(1) octahedra share an edge formed by O(9) and O(12). Whereas O(9) implies short distances [Co(4)–O(9) 2.092 Å and Co(1)–O(9) 2.074 Å], O(12) corresponds to weaker bonds [Co(4)–O(12) 2.170 Å and Co(1)–O(12) 2.129 Å]. That means that the coupling will be stronger via O(9) than via O(12). The exchange angles corresponding to the "strong" exchange pathway are close to 100° (Co(4)–O(9)–Co(1) 100.4° ; Co(1)–O(5)–Co(3) 99.5°) (Figure 8). In contrast, for the "weak" exchange pathways the angles are

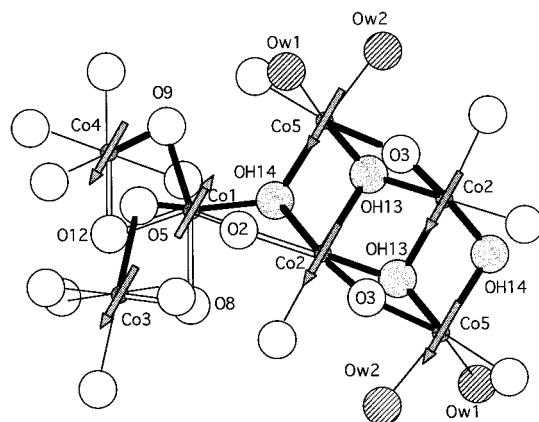


Figure 8. Possible model of the magnetic structure. The strong and weak 90° exchange pathways are indicated as large black and empty sticks, respectively. The magnetic moments are symbolized by arrows.

respectively Co(4)–O(12)–Co(1) 96.2° and Co(3)–O(8)–Co(1) 96.9° . The strong interactions corresponding to the larger angles are therefore antiferromagnetic. The same analysis applied to the tetrameric unit shows angles close to 97° . These geometrical constraints applied to the evolution of the exchange constant J with the superexchange angles are in agreement with weak antiferromagnetic coupling along the chains associated with weak ferromagnetic coupling within the tetrameric unit. In this case, the blank angle is in the 98 – 99° range. Moreover, the interactions between the chain and the cluster are governed by the Co(1)–OH(14)–Co(5) pathway since these two octahedra share only one vertex. The corresponding exchange angle (121.91°) implies antiferromagnetic coupling and allows proposing the possible magnetic structure presented in Figure 8.

Conclusion

The solid can be considered as a stacking of metal oxide layers that form 14-membered ring channels linked by the alkyl chains of the succinate anions. The water molecules present in the channels can be removed without losing the crystallinity of the solid, which suggests the possibility of using the porosity of the material by easily removing the water. With the utilization of the hydrothermal technique, we have demonstrated that dicarboxylate can be used to make compounds that present two advantages: a nontemplated structure and an infinite array of Co^{2+} octahedra associated with ferrimagnetic properties. The structure of the anhydrous phases and the study of their porosity are currently in progress.

Acknowledgment. We are very grateful to Marc Nogues, from the Laboratoire de Magnétisme et d'Optique, Université de Versailles St-Quentin, for magnetic measurements.

Supporting Information Available: Crystal data and structure refinement, atomic coordinates and equivalent isotropic displacement parameters, bond lengths and angles, anisotropic displacement parameters, hydrogen coordinates and isotropic displacement parameters, and observed and calculated structure factors for $\text{Co}_4(\text{OH})_2(\text{H}_2\text{O})_2(\text{C}_4\text{H}_4\text{O}_4)_3 \cdot 2\text{H}_2\text{O}$. This material is available free of charge via the Internet at <http://pubs.acs.org>.

CM980781R

(18) Férey, G. Unpublished results.

(19) Clemente, J. M.; Andres, H.; Aebersold, M.; Borrás-Almenar, J. J.; Coronado, E.; Güdel, H. U.; Büttner, H.; Kearly, G. *Inorg. Chem.* **1997**, *36*, 2244.

(20) Aebersold, M.; Andres, H.; Büttner, H.; Borrás-Almenar, J. J.; Clemente, J. M.; Coronado, E.; Güdel, H. U.; Kearly, G. *Physica B* **1997**, *234*, 764.

(21) Goodenough, J. B. *Magnetism and the chemical bonds*; Wiley-Interscience: New York, 1963.